JOURNAL OF MAGNETIC RESONANCE IMAGING 36:1273–1286 (2012)

Review

Time-Resolved Angiography: Past, Present, and Future

CME

Thomas M. Grist, MD,[1] Charles A. Mistretta, PhD,[1,2] Charles M. Strother, MD,[1*] and Patrick A. Turski, MD[1]

This article is accredited as a journal-based CME activity. If you wish to receive credit for this activity, please refer to the website: www.wileyhealthlearning.com

ACCREDITATION AND DESIGNATION STATEMENT

Blackwell Futura Media Services designates this journal-based CME activity for a maximum of 1 *AMA PRA Category 1 Credit*™. Physicians should only claim credit commensurate with the extent of their participation in the activity.

Blackwell Futura Media Services is accredited by the Accreditation Council for Continuing Medical Education to provide continuing medical education for physicians.

EDUCATIONAL OBJECTIVES

Upon completion of this educational activity, participants will be better able to discuss the evolution in methods for time-resolved angiography including the rapid acceleration of angiographic methods to combine high spatial and temporal resolution while preserving SNR.

ACTIVITY DISCLOSURES

No commercial support has been accepted related to the development or publication of this activity.

Faculty Disclosures:

The following contributors have no conflicts of interest to disclose:

Editor-in-Chief: C. Leon Partain, MD, PhD

CME Editor: Scott B. Reeder, MD, PhD

CME Committee: Scott Nagle, MD, PhD, Pratik Mukherjee, MD, PhD, Shreyas Vasanawala, MD, PhD, Bonnie Joe, MD, PhD, Tim Leiner, MD, PhD, Sabine Weckbach, MD, Frank Korosec, PhD

Authors: Thomas M. Grist, MD, Charles A. Mistretta, PhD, Charles M. Strother, MD, and Patrick A. Turski, MD

This manuscript underwent peer review in line with the standards of editorial integrity and publication ethics maintained by *Journal of Magnetic Resonance Imaging*. The peer reviewers have no relevant financial relationships. The peer review process for *Journal of Magnetic Resonance Imaging* is double-blinded. As such, the identities of the reviewers are not disclosed in line with the standard accepted practices of medical journal peer review.

Conflicts of interest have been identified and resolved in accordance with Blackwell Futura Media Services's Policy on Activity Disclosure and Conflict of Interest. No relevant financial relationships exist for any individual in control of the content and therefore there were no conflicts to resolve.

INSTRUCTIONS ON RECEIVING CREDIT

For information on applicability and acceptance of CME credit for this activity, please consult your professional licensing board.

This activity is designed to be completed within an hour; physicians should claim only those credits that reflect the time actually spent in the activity. To successfully earn credit, participants must complete the activity during the valid credit period.

Follow these steps to earn credit:

- Log on to www.wileyhealthylearning.com
- Read the target audience, educational objectives, and activity disclosures.
- Read the article in print or online format.
- Reflect on the article.
- Access the CME Exam, and choose the best answer to each question.
- Complete the required evaluation component of the activity.

This activity will be available for CME credit for twelve months following its publication date. At that time, it will be reviewed and potentially updated and extended for an additional period.

[1]Department of Radiology, University of Wisconsin School of Medicine and Public Health, Madison, Wisconsin, USA.
[2]Department of Medical Physics, University of Wisconsin School of Medicine and Public Health, Madison, Wisconsin, USA.
*Address reprint requests to: C.M.S., Department of Radiology, 1111 Highland Ave., Madison, WI, 53792. E-mail: cstrother@uwhealth.org
Received October 1, 2011; Accepted February 17, 2012.
DOI 10.1002/jmri.23646
View this article online at wileyonlinelibrary.com.

The introduction of digital subtraction angiography (DSA) in 1980 provided a method for real time 2D subtraction imaging. Later, 4D magnetic resonance (MR) angiography emerged beginning with techniques like Keyhole and time-resolved imaging of contrast kinetics (TRICKS) that provided frame rates of one every 5 seconds with limited spatial resolution. Undersampled radial acquisition was subsequently developed. The 3D vastly undersampled isotropic projection (VIPR) technique allowed undersampling factors of 30–40. Its combination with phase contrast displays time-resolved flow dynamics within the cardiac cycle and has enabled the measurement of pressure gradients in small vessels. Meanwhile similar accelerations were achieved using Cartesian acquisition with projection reconstruction (CAPR), a Cartesian acquisition with 2D parallel imaging. Further acceleration is provided by constrained reconstruction techniques such as highly constrained back-projection reconstruction (HYPR) and its derivatives, which permit acceleration factors approaching 1000. Hybrid MRA combines a separate phase contrast, time-of flight, or contrast-enhanced acquisition to constrain the reconstruction of contrast-enhanced time frames providing exceptional spatial and temporal resolution and signal-to-noise ratio (SNR). This can be extended to x-ray imaging where a 3D DSA examination can be used to constrain the reconstruction of time-resolved 3D volumes. Each 4D DSA (time-resolved 3D DSA) frame provides spatial resolution and SNR comparable to 3D DSA, thus removing a major limitation of intravenous DSA. Similar techniques have provided the ability to do 4D fluoroscopy.

Key Words: angiography; advanced imaging; MRA; DSA; CTA
J. Magn. Reson. Imaging 2012;36:1273–1286.

SOON AFTER HARVEY'S DESCRIPTION in 1628 of the continuous flow of blood throughout the body, the need for methods that would allow patterns, distributions, and rates of blood flow to be visualized and quantified was recognized. It was not, however, until after discovery of the x-ray over 200 years later that pioneers from various backgrounds and countries began to systematically explore ways in which these dynamic features of the circulation could be recorded and quantified in humans. Progress was quick and, only some 30 years after Roentgen's discovery, the availability of mechanical film changers, mechanical pressure injectors, and relatively nontoxic iodinated contrast media converged so that investigators could begin to perform clinically relevant angiographic studies (1–3). Additional technologic advances rapidly followed and, by the middle of the 20th century automatic film cassette changers, image intensifiers, improved catheter materials, and a simple and safe method of gaining percutaneous access to the vascular system were widely available; x-ray angiography was established as a fundamental tool in the clinical and experimental study of the vasculature.

X-RAY ANGIOGRAPHY BEFORE DIGITAL SUBTRACTION ANGIOGRAPHY (DSA)

Shortly before the introduction of computed tomography (CT) in 1972, x-ray angiography had evolved to a stage where diagnostic angiograms were a routine part of daily routine in most radiology departments. Film changers had improved so that angiographic acquisitions of many seconds could be recorded at high frame rates; contrast medium had evolved so that it was much safer than that previously available, photographic subtraction, angiotomography, and magnification angiography had been described, and refined improvements in catheter materials and techniques had evolved to a degree that adverse events had become relatively uncommon. In spite of these significant improvements, angiographic procedures were still significantly limited by several factors. Perhaps most important among these was the time, contrast medium dose, and radiation exposure that was often required to achieve an image series that clearly displayed relevant vascular anatomy. First, a standard single plane (or biplane if available) acquisition was acquired. Films were removed from the film changer, taken to the darkroom, developed, and, often, photographic subtraction of key images was performed; the time from an acquisition to viewing of the images by physicians took as long as 20–30 minutes. Frequently, it was necessary to obtain one or more additional acquisitions, each done with a different projection requiring, each time, an additional contrast medium injection, radiation exposure, and time for film development and processing. A comprehensive angiographic study of the intracranial vessels could thus easily require 2 hours or more for completion.

DIGITAL SUBTRACTION ANGIOGRAPHY (DSA)

In the early 1970s investigators at the University of Wisconsin (4) were experimenting with a dual silicon target storage tube system that was used in combination with a spinning filter wheel and peak kilovoltage (kVp) switching to perform 3-spectrum K-edge imaging of iodine. Due to the many adjustments needed to tune this analog system, work began in 1976 on a digital video image processor (5) that would permit real-time adjustment of the image weightings needed to cancel bone and soft tissue after a single x-ray exposure. Inspired by work at the University of Arizona using offline processing of time subtraction angiographic data (6), the University of Wisconsin group turned their attention to real-time processing of angiographic data acquired with intravenous injections (7,8). The technique provided a real-time series of subtraction images during the passage of contrast and was initially named Computerized Fluoroscopy. The "digital subtraction angiography" or simply "DSA" label was eventually suggested by Dr. Tom Meany from Cleveland Clinic.

Because of the advantages of digital processing, it was originally hoped that DSA would provide a means by which high-quality angiography could be performed using an intravenous (IV) injection of contrast medium, thus reducing both the discomfort and the incidence of complications that were associated with direct intraarterial injections. Rather quickly, however, it became apparent that the IV DSA technique was limited by the

fact that, even with biplane acquisitions, there were often problems due to suboptimal viewing angles and vessel overlap that could only be eliminated by repeated injections (and even then only if a projection could be defined that would avoid overlap of relevant vascular structures). Also, because of the limited amount of iodine signal associated with the IV injection of contrast medium, adequate image quality of IV DSA was dependent on there being both an adequate cardiac output and minimal patient motion. For these reasons, IV DSA was rather rapidly replaced by techniques that combined digital processing with standard intraarterial angiographic examinations.

Nevertheless, because it allowed a significant reduction in both the time necessary to perform an angiographic examination and the amount of contrast medium that was required, the availability of DSA resulted in a significant reduction in the adverse events associated with angiography. Over the ensuing 30 years, steady advancements in both hardware and software have resulted in an improvement in DSA capability so that now it can provide exquisite depiction of the vasculature in both 2D and rotational 3D formats (9,10).

MAGNETIC RESONANCE ANGIOGRAPHY (MRA)

The earliest MRA sequences were noncontrast-enhanced sequences relying on phenomena like systole/diastole phase differences (11), inflow (12–14), or flow generated phase differences (15). Following the introduction of gadolinium to enhance T1 contrast (16), a progression of nontime-resolved contrast-enhanced techniques evolved, permitting high-resolution 3D MRAs in times typically on the order of 30 seconds. Methods such as bolus detection (17,18), MR fluoro triggering (19), and elliptical centric phase encoding (20) were developed to ensure that the central portion of *k*-space was filled during periods of adequate contrast. Basic improvements in MR data acquisition, including radiofrequency (RF)-spoiled FLASH sequences (21), were employed to increase speed and provide optimal T1 contrast.

In spite of these advances, bolus timing remained an issue and there was a desire to increase temporal resolution so that dynamic vascular phenomena could be assessed. This led to the development of time-resolved MRA.

TIME-RESOLVED MRA

Keyhole Imaging

In the late 1980s, methods for time-resolved angiography began to emerge using MRI. These techniques generally provided less spatial and temporal resolution than DSA but offered time-resolved 3D sets following IV injection. These techniques took advantage of the ability of MRI to selectively sample different regions of *k*-space and to take advantage of the fact that the central portion of *k*-space is dominant in determining image contrast. The keyhole method of Van Vaals et al (22) generated a time series of images by combining rapidly acquired temporal samples of the central *k*-space region with a single sample of the outer regions of *k*-space, typically obtained at the end of the scan. While providing some sense of the dynamics of the evolving contrast in the vessels, high spatial frequency venous signals appear even in the early arterial frames due to the combination of the late high spatial frequency information.

TRICKS

In 1998, the time-resolved imaging of contrast kinetics (TRICKS) technique was introduced by Korosec et al (23). In this method the central portion of *k*-space is sampled more frequently than the peripheral regions and time frames are formed by temporal interpolation. This represented a significant improvement over the keyhole method due to the ongoing updating of high spatial frequency information. This technique and its derivatives are currently the most prevalent commercial methods for time-resolved MRA. However, although good dynamic studies can be performed, especially when augmented by parallel imaging techniques, spatial resolution is limited and although frames may be updated every few seconds, the data used to form each time frame cover a substantial temporal interval of ten seconds or more due to the temporal interpolation that is required.

Undersampled 2D Radial MRA

In an attempt to increase the spatial and temporal resolution provided by traditional Cartesian acquisition, where resolution is proportional to the number of excitations, Peters et al (24) investigated the use of undersampled 2D radial acquisition. These methods had been investigated by Rasche et al (25) for catheter tracking and by Scheffler and Hennig (26) for small field of view (FOV) imaging. The latter study pointed out that when radial acquisition is undersampled there is a small FOV in which resolution depends only on the number of readout samples and not on the number of projections. Beyond this small FOV, streak artifacts begin to appear and communicate with distant portions of the image. Peters et al hypothesized that for the purposes of MRA, where the dataset is exceptionally sparse, these artifacts might be tolerable and allow faster acquisition in which spatial resolution would not be proportional to the number of excitations. It was found that typical radial undersampling factors of about four relative to the Nyquist criterion resulted in acceptable artifact levels with significant improvements in spatial resolution relative to Cartesian acquisition.

Undersampled Radial 3D Vastly Undersampled Isotropic Projection (VIPR)

Shortly thereafter, Barger et al (27) extended radial undersampling to three dimensions using VIPR. When undersampling is done in 3D the artifacts are more effectively dispersed and play a lesser role than in 2D. Undersampling factors for angiographic applications

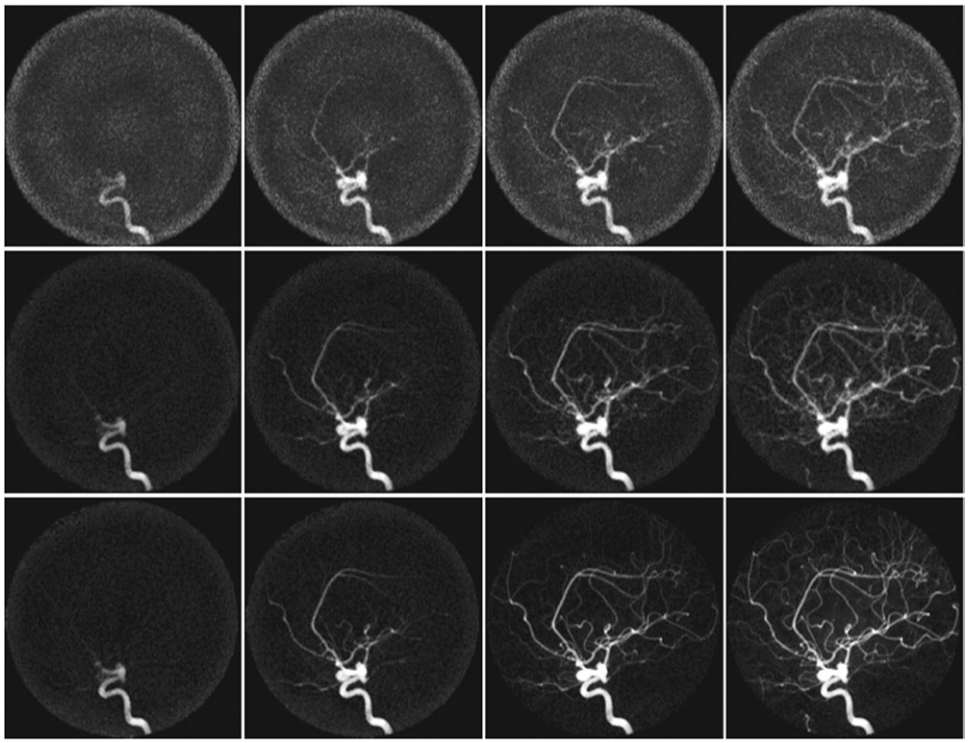

Figure 1. Comparison of three techniques: Iterative Sense (top row), Iterative Sense + Compressed Sensing using L0 minimization (middle row), and the combination of both of these with HYPR (bottom row). Courtesy of Velikina and Samsonov (43).

are typically 30 or more. Time-resolved series of VIPR images are used in conjunction with a temporal tornado filter that reconstructs images using a spatial frequency-dependent temporal window that is typically on the order of 1 second or less at the center of *k*-space and increases to a few seconds at the highest spatial frequencies, thus incorporating some of the strategy of the TRICKS sequence while supplying far more spatial resolution in a given time interval. VIPR has been extensively studied using a phase contrast readout sequence which, when used with Navier-Stokes analysis, has permitted measurement of vascular pressure gradients and estimates of wall shear stress (28–30; Bley TA et al, unpubl. data). This has been made possible by an order of magnitude decrease in voxel size relative to previous implementations of phase contrast using Cartesian trajectories.

Constrained Reconstruction

Any accelerated technique can suffer from increased artifacts and a loss of signal-to-noise ratio (SNR) in proportion to the square root of the acceleration factor. Recently, the highly constrained back-projection reconstruction (HYPR) technique (31), related to the constrained reconstruction techniques introduced by Webb et al (32) 20 years ago, has been applied to time-resolved MRA and a broad range of medical imaging applications (33–36). The main idea of this approach is that in a medical image series there is often a sequence of images that have correlated spatial information with each image in the sequence corresponding to some parameter like time, echo time, inversion time, diffusion value, diffusion direction, etc. A composite image is typically formed from all or a subset of images from the series and is used to constrain the reconstruction of the images associated with each value of the image parameter. For time-resolved MRA, in the absence of motion, it is typical to form the composite from a sum of time frames. The individual time frame is formed by convolving the individual undersampled time frames to form a weighting image that is used to extract that portion of the composite that is present at each point in time. Because of the convolution, the SNR of the reconstructed time frame is typically close to that of the composite, as is the spatial resolution. This process greatly reduces the traditional tradeoff between spatial and temporal resolution.

There are now several variations of the HYPR algorithm (37–40) that can be used in situations where sparsity is not as favorable as in angiography. Many of these involve iterative reconstruction which, given the speed of present computers, is not a serious limitation.

When HYPR is combined with VIPR acquisition, acceleration factors as large as 1000, relative to traditional unaccelerated Cartesian imaging, have been achieved, as demonstrated later.

Compressed Sensing

Recently, Candes et al (41) produced an alternative to the traditional Nyquist theorem that points out that we do not need n^3 measurements to solve for n^3 voxel values if the image data are sparse and the noise is incoherent. By iteratively minimizing various image norms subject to data consistency constraints, it is possible to generate accelerations on the order of 10 or less using compressed sensing reconstructions (42). These methods are generally complementary to the accelerations achieved with VIPR and HYPR and can be used in conjunction with these methods to

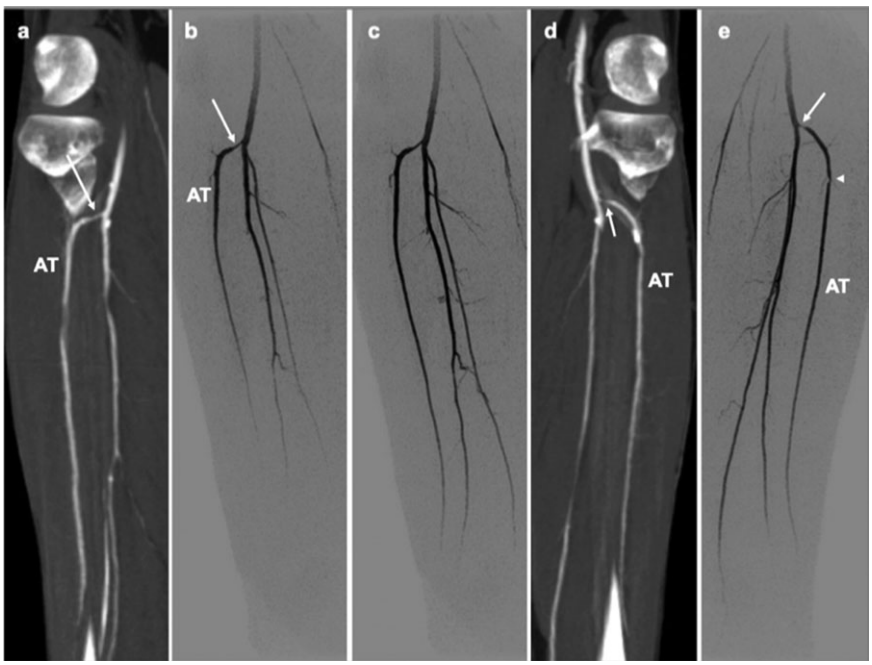

Figure 2. Comparison of MR angiographic with CT angiographic results in patient suspected of having peripheral vascular disease. Only subvolumes of full FOV CT and MR angiographic results are shown. **a**: Slightly oblique coronal reformation of right leg from CT angiography. A stenosis is identified at the origin of the right anterior tibial artery (AT) (arrow). **b,c**: Maximum intensity projections (MIPs) from two consecutive time frames of MRA of the same region as seen on CT angiographic result in (a) also show stenosis (arrow). **d**: Slightly oblique coronal reformation of left leg from CT angiography. A stenosis is identified at the origin of the left anterior tibial artery (arrow). **e**: MIP from one time frame of MR angiography of the same region as seen on CT angiographic result in (d) also shows stenosis (arrow), as well as another stenosis distally (arrowhead). Figure and caption courtesy of Stephen Riederer (44).

further reduce artifacts and thus permit even higher accelerations. These methods can be further enhanced using parallel imaging, leading to exciting possibilities for new applications that previously could not be contemplated due to time constraints.

It is interesting to note that the VIPR angiographic acquisition, while satisfying conditions for compressed sensing methodology, intrinsically produces greater acceleration than would the application of compressed sensing methods.

Image quality improves when several acceleration methods are employed (Fig. 1) (43). In this study, time frames were generated using 10 projections, representing an undersampling factor of 40. Iterative SENSE reconstruction was employed followed by compressed sensing using L0 minimization and then HYPR. Images formed with SENSE and compressed sensing exhibit lower spatial resolution and SNR than the images formed using the combination of all three techniques.

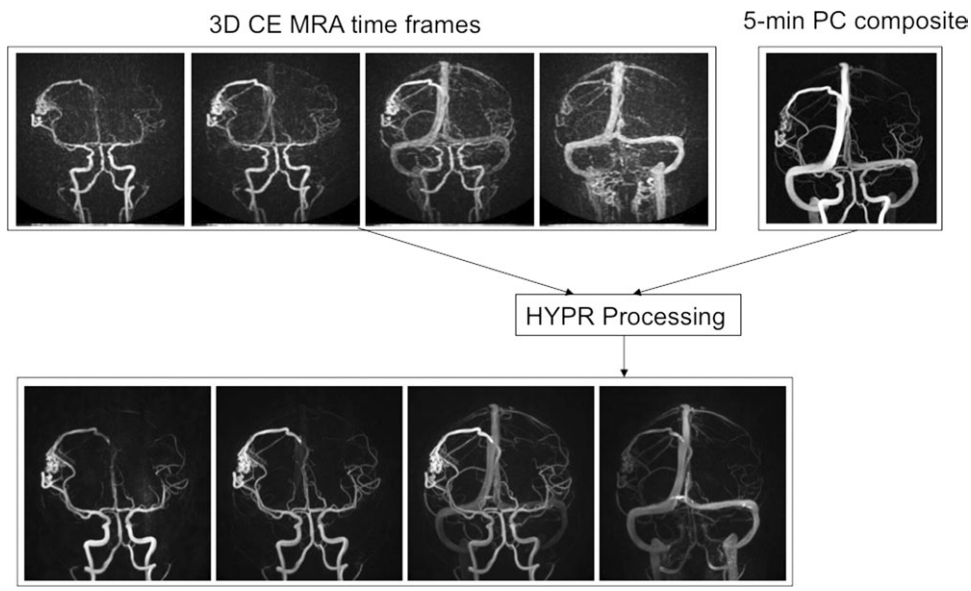

Figure 3. Illustration of Hybrid HYPR MRA. Serial 3D radial scans are obtained during the first pass of a contrast bolus. Following the dynamic imaging a separate composite image is generated from a scan with a longer acquisition time, in this example a phase contrast scan. The phase contrast exam is used to constrain the generation of time frames using HYPR resulting in improved image quality (bottom row).

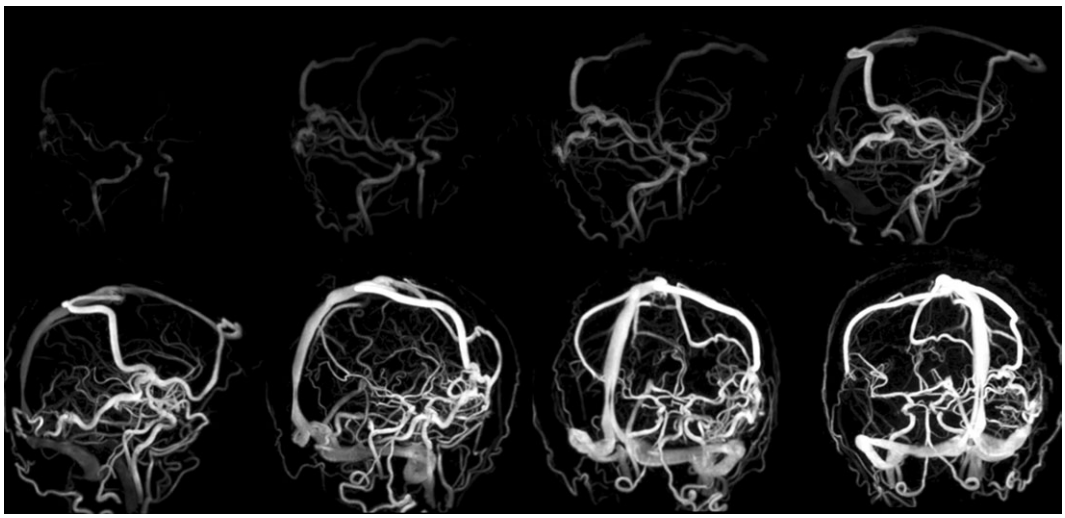

Figure 4. Selected frames from a hybrid phase contrast HYPR MRA series of a temporal lobe arteriovenous malformation of the brain. Each frame was rotated 20° to demonstrate the 4D features of the exam. Voxel size: 0.33 mm^3; temporal resolution: 0.75 seconds; frame time and temporal window of contrast-enhance information: 0.75; undersampling factor: 800 relative to the radial Nyquist sampling requirement associated with the achieved spatial resolution. Note the excellent delineation of the cortical venous drainage (arrows). (Images courtesy of Yijing Wu, PhD.)

Highly Accelerated Cartesian MRA

Recently, highly accelerated Cartesian implementation has been made possible using 2D parallel imaging (Fig. 2). In the Cartesian acquisition with projection reconstruction (CAPR) sequence (44), phase encodings are arranged in a radial distribution. Readout is in the through-plane direction. The density of these phase encodings can be sparse, as in the Peters et al undersampled 2D radial method. This combined with large parallel imaging acceleration factors has enabled acceleration factors on the order of 50. The method has recently been combined with a compressed sensing algorithm (45), which helps restore SNR loss that accompanies accelerated imaging.

The real-time reconstruction of CAPR images has been employed to trigger table motion in two-station peripheral angiography of the thighs and calves (46). Purely arterial time-resolved frames with minimal venous contamination are acquired in both stations.

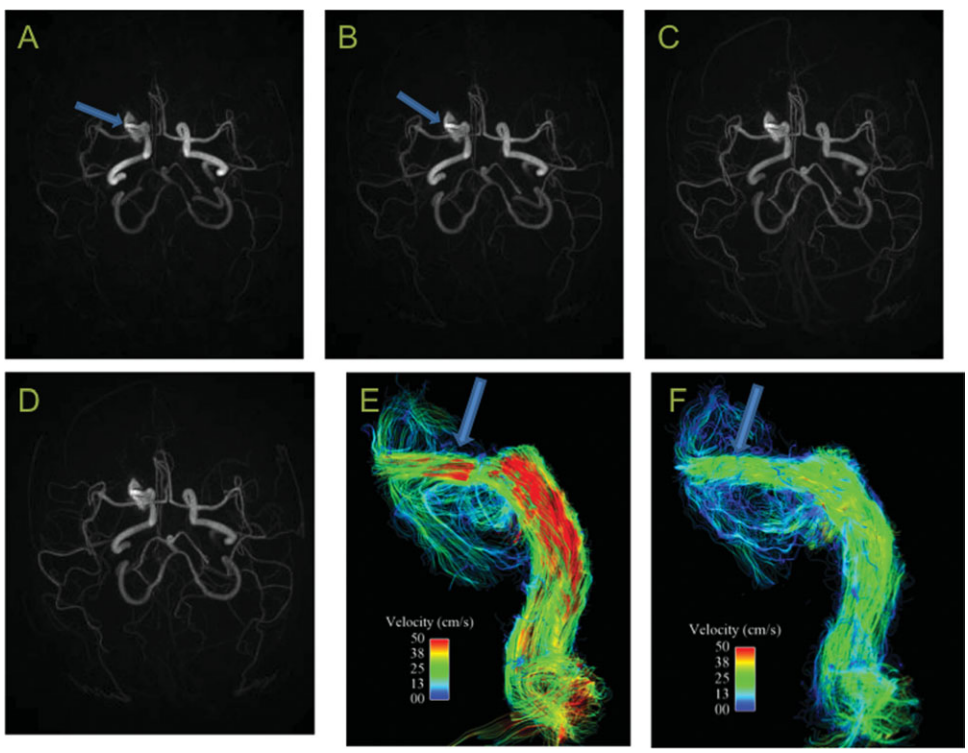

Figure 5. Right internal carotid aneurysm. The early arterial frames identify an inflow jet (arrow) and slower recirculating flow along the wall of the aneurysm. The streamline images show the inflow jet, impact zone, and slow flow regions during systole and diastole. (Images courtesy of Yijing Wu, PhD, and Ben Landgraf.)

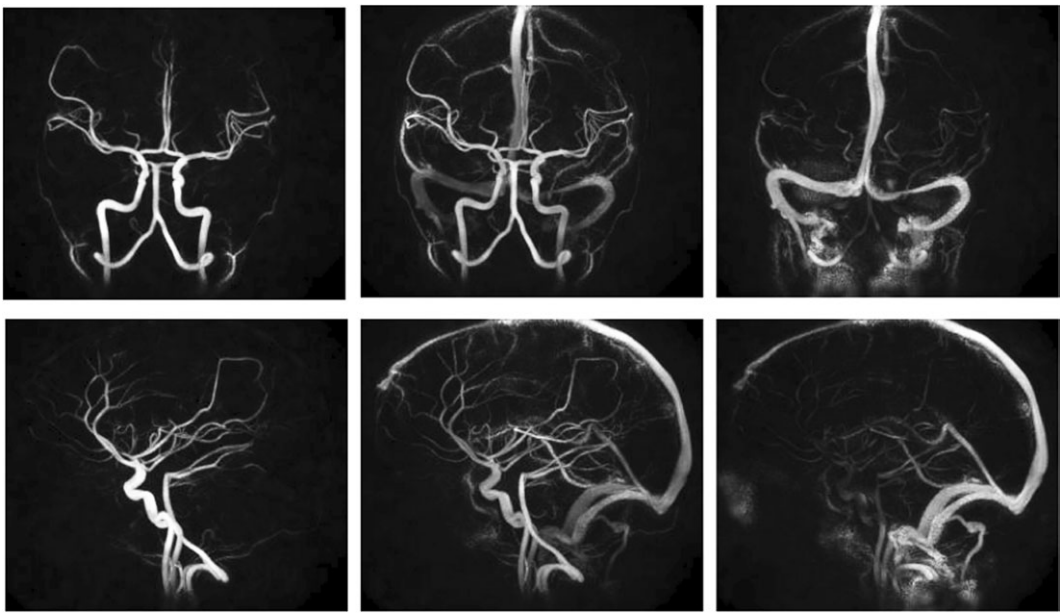

Figure 6. PC Hybrid HYPR images obtained with 1 cc of contrast. Representative arterial, mixed, and venous time frames from a 60-frame series. Spatial resolution is 0.69 mm isotropic with 0.75 seconds temporal resolution. (Images courtesy of Yijing Wu, PhD.)

Wang et al (47) used HYPR in connection with a 3D time-resolved Cartesian acquisition employing random phase encoding in-plane and through-plane readout. This method produces good temporal resolution and significant SNR increases relative to conventional unconstrained reconstruction.

Hybrid HYPR MRA

The idea of using a composite image formed from the series of time frames following contrast injection can be modified to include the generation of a composite image from a separate scan of longer duration. For example, a phase contrast scan or a time-of-flight scan can be done before or after the dynamic contrast scan to generate a HYPR composite of very high SNR and spatial resolution (48,49). The combined use of this kind of composite and the contrast-enhanced scan decouples the spatial and temporal resolution and eliminates the traditional tradeoff between these attributes (Fig. 3).

A hybrid HYPR exam was performed using a phase contrast (PC) composite image as the constraint to display the filling dynamics of a patient's superficial temporal lobe arteriovenous malformation (AVM) (Fig. 4). The resultant spatial resolution of 0.69 mm isotropic provided rapid enhancement of the cortical venous drainage of the temporal lobe arteriovenous malformation and showed it was due to shunting through the AVM nidus.

The phase contrast acquisition used for HYPR reconstruction was also cardiac-gated and provided quantitative measurements of blood flow velocity

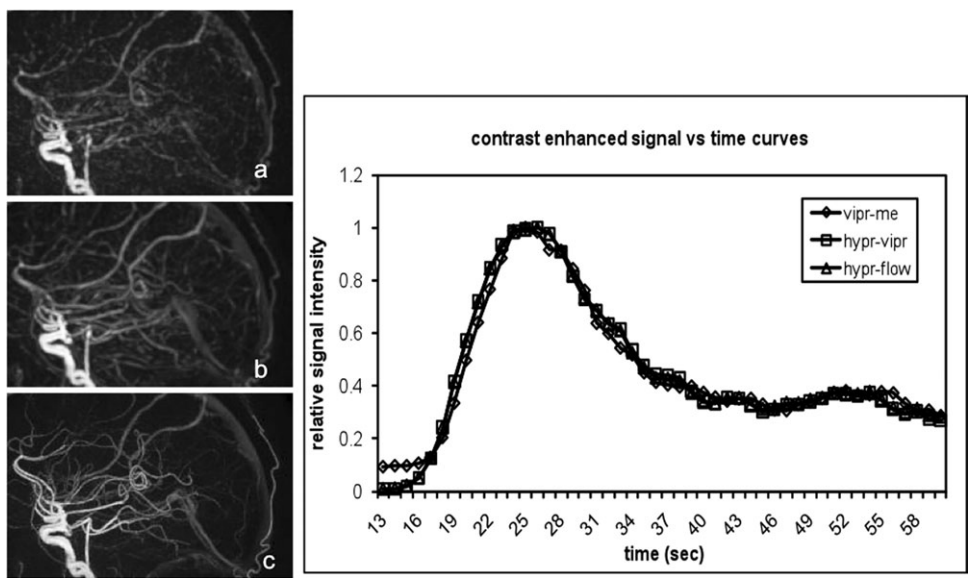

Figure 7. Progression of VIPR image quality obtained by using HYPR reconstruction. (**a**) Source image from the CE VIPR time series, (**b**) CE VIPR + HYPR using a composite of all the time frames as the constraint, and (**c**) same time frame using a phase contrast scan as the composite image. (Images courtesy of Yijing Wu, PhD.)

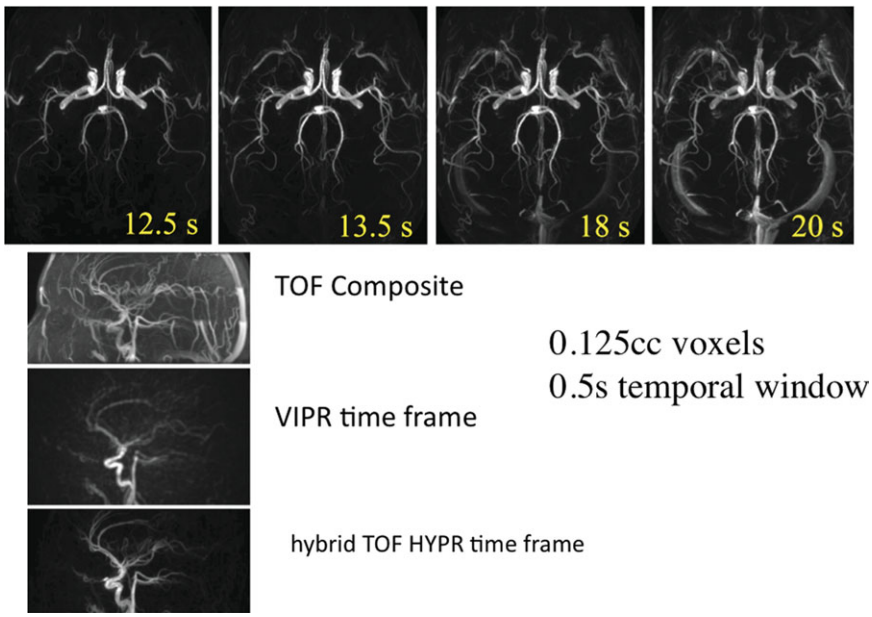

Figure 8. Selected frames for hybrid TOF study. The isotropic voxel size is 0.125 mm^3 with a 0.5-second temporal window for all contrast enhanced information including a tornado filter. (Images courtesy of Yijing Wu, PhD.)

throughout the cardiac cycle in a third patient (Fig. 5), which was very useful in treating a carotid aneurysm. This technique provided an improved SNR that produced high-quality images with a lower dosage of contrast material (Fig. 6). Image quality of a basic VIPR time series was improved with the use of a tornado filter (27), HYPR processing, and the hybrid technique with a phase contrast composite (Fig. 7). The increased image quality using the hybrid technique is evident.

If a time-of-flight (TOF) composite is used, the time normally spent in phase contrast for flow encoding can be used to generate higher spatial resolution (Fig. 8) (Wu Y, et al, submitted to JMRI).

Figure 9 summarizes the degrees of acceleration that have been achieved with various techniques, beginning with the present commercial time-resolved technique (TRICKS and related methods) progressing through to those employing increasing degrees of parallel imaging, undersampling, and constrained reconstruction.

Time-Resolved Noncontrast Inflow Techniques

Recent concerns regarding nephrotoxic systemic fibrosis have stimulated the development of noncontrast-enhanced spin-labeled inflow techniques. The progress in this area deserves a separate review article. We will only provide a brief outline of these developments here.

Several variations of nontime-resolved noncontrast-enhanced techniques have been introduced. These include fresh blood inflow sequences that subtract systolic and diastolic acquisitions (50) and magnetization prepared sequences in which an inversion pulse is used to identify blood flowing into or out of an imaging region (51). Subtractive spin labeling techniques employing sequences with two different preparation pulses have also provided promising results. These are typically 3D sequences and are subject to motion and potential variations in the optimal readout delay, depending on pathology and patient-to-patient flow variations. Edelman et al (52) recently introduced the QISS technique, which is a sequential 2D slice

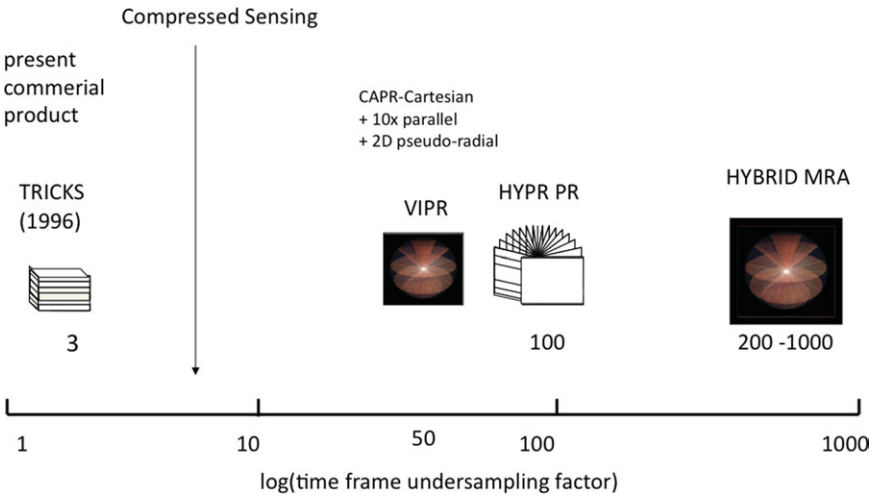

Figure 9. Representative accelerations achieved using various MRA methods.

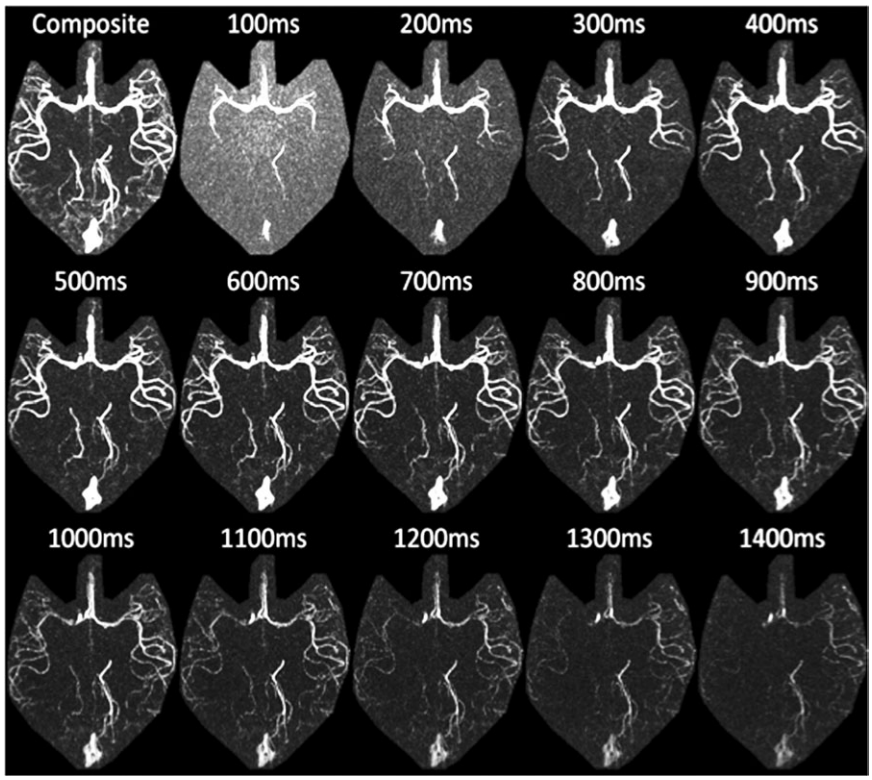

Figure 10. Time-resolved inflow with subtractive balanced SSFP using radial trajectories. This approach has the advantage of high temporal resolution (100 msec) and does not require the injection of contrast material (no bolus dispersion). The resolution in this example is 1.0 mm isotropic and the scan time is 6 minutes. (Images courtesy of Kevin Johnson, PhD.)

technique tolerant of motion and spatial variations in inflow. This sequence has provided excellent results and appears to be clinically robust.

Spin-labeling techniques, typically employing a subtraction of a noninverted and an inverted tag, have been extended to provide temporal resolution by varying the inflow delay following magnetization preparation (53–58). One of the attractive features of these techniques relative to contrast-enhanced MRA is the absence of the bolus dispersion associated with IV contrast injection. This makes these sequences attractive for cases in which high temporal resolution may be required. However, since the acquisition typically takes several minutes, motion can be a problem. Johnson et al (57,58) recently reported the combination of VIPR with a subtractive spin labeled sequence that provides 0.7 mm isotropic resolution and time-resolution on the order of 70 msec (Fig. 10).

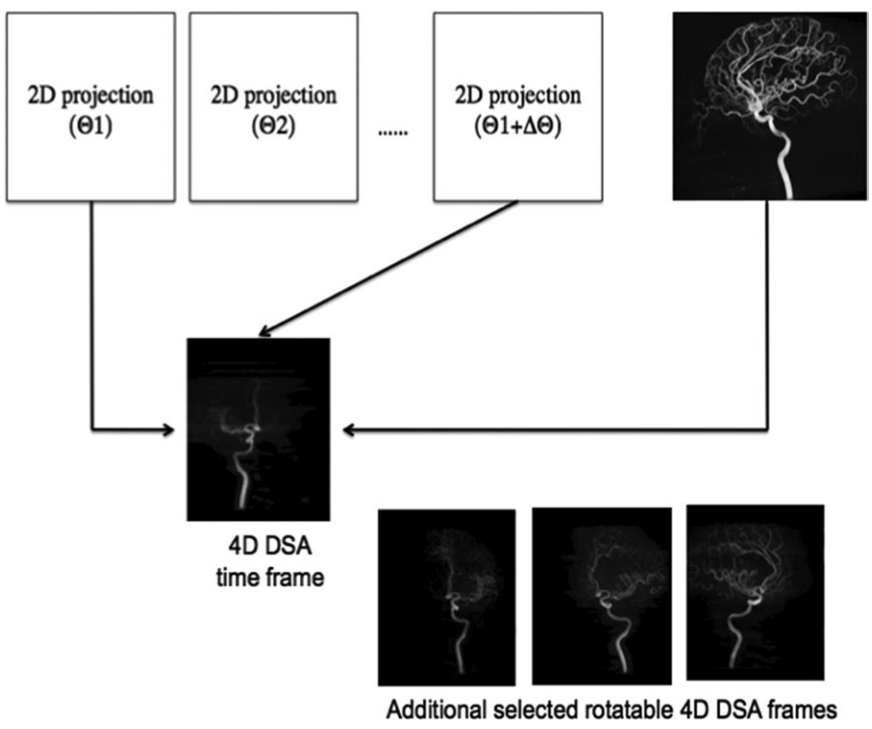

Figure 11. Schematic of the two projections used in 4D DSA reconstruction.

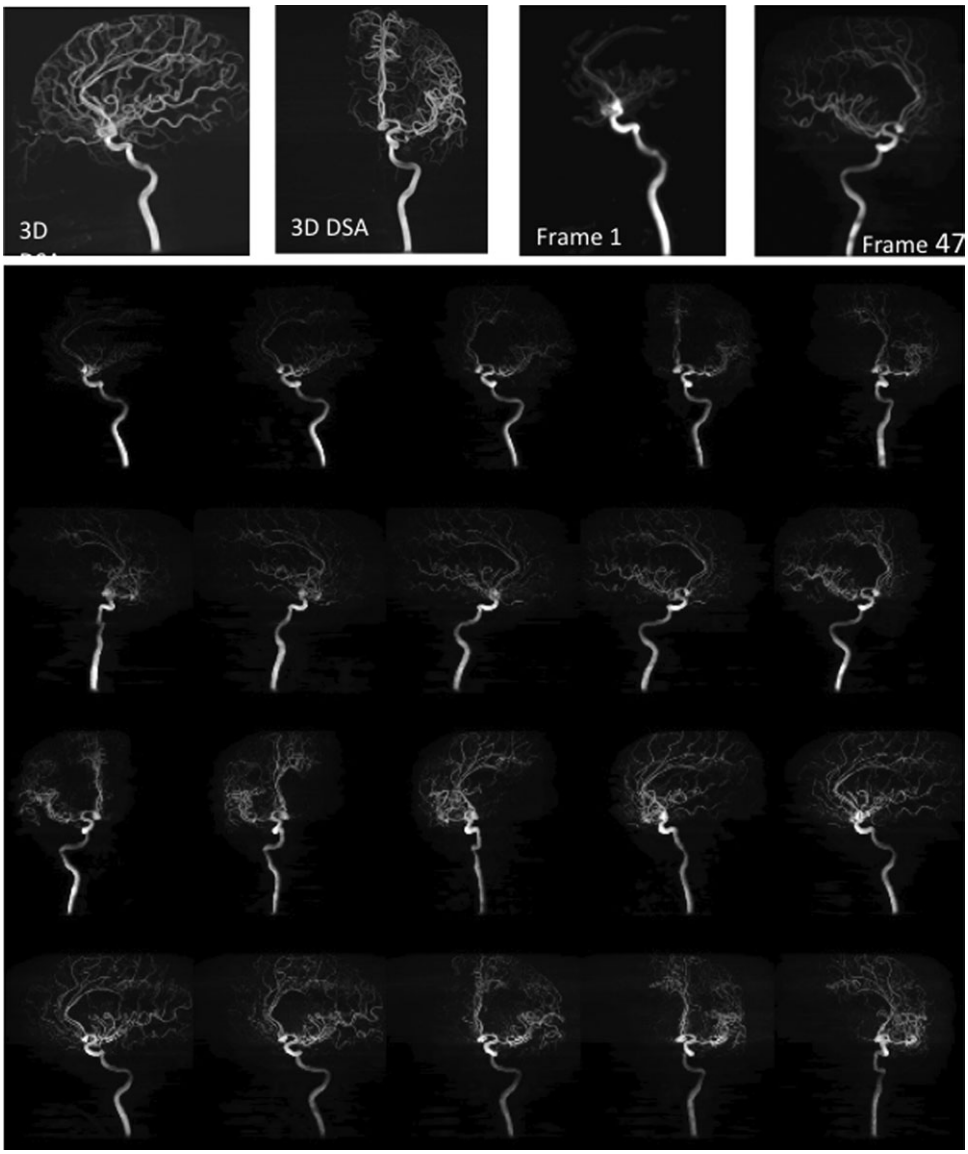

Figure 12. Two views of 3D rotational DSA reconstruction, frames 1 and 47 and selected MIPS through the 4D DSA time-resolved volumes.

4D DSA

While CT DSA may provide time-resolved 3D data sets using multiple subsecond gantry rotations with wide area CT detectors (59), these systems are not well suited to interventional work and it would be advantageous to be able to generate time-resolved 3D data sets using cone beam interventional systems.

The ideas of constrained reconstruction can be extended to x-ray DSA on cone beam interventional systems to produce 3D volumes at higher frame rates than possible with rapid gantry rotation (60). These systems presently produce 2D projection images and 3D volumes at a rate of one volume per several seconds. The algorithms used for 4D DSA differ significantly from the MRA algorithms where a well-sampled 3D image volume is used to constrain the reconstruction of a series of contrast-enhanced 3D time frames of lower SNR and resolution. In the 4D DSA x-ray case, a rotational DSA image volume is typically used in conjunction with just two 2D projection images separated in time. The use of two projections appears to be adequate to resolve shadowing artifacts in which back-projected arterial intensity might be deposited in undesired vessels that might line up in a single projection. Figure 11 shows a schematic of the images used in the reconstruction.

Figure 12 shows two rotational 3D DSA views that contain no temporal information. Selected rotating time frames are also shown along with separate images of frames 1 and 47.

Contrast waveforms generated from the reconstructed 4D DSA time frames agree well with those obtained from the 2D projection information (Fig. 13).

For cerebral angiography, 4D DSA potentially provides substantially higher spatial and temporal resolution than all competing techniques (Fig. 14). However, the temporal resolution of 4D DSA requires some explanation. When just two projections are used to form time frames, a vessel that does not fill until the time of the second projection can appear at the earlier time if it lines up with an early filling vessel in the first projection.

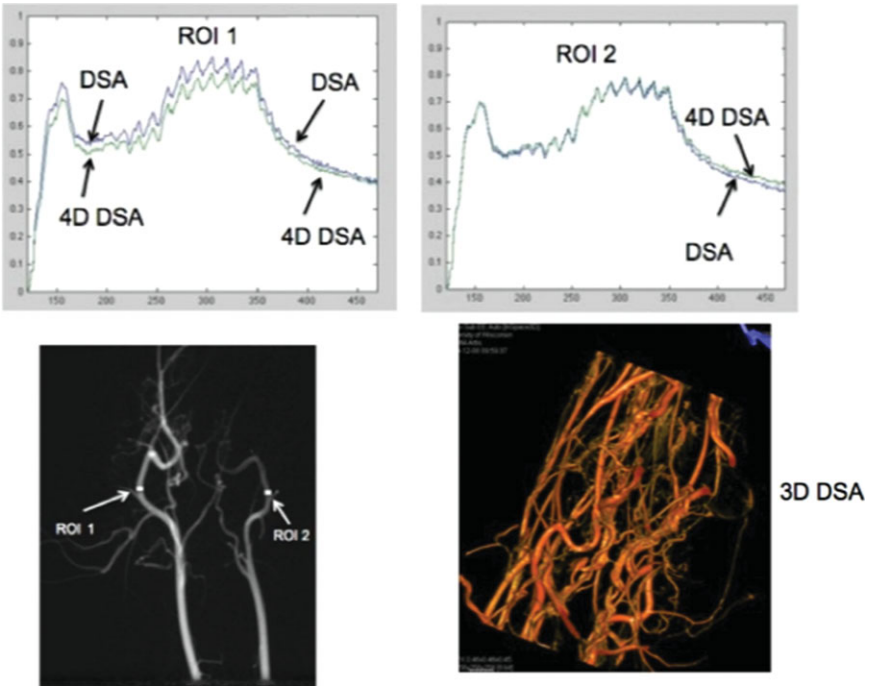

Figure 13. Comparison of flow curves obtained from fixed angle 2D projections (lower left) at 48° below lateral and corresponding regions of interest in a reconstructed AP view through the 4D DSA image volume. The curves have been slightly offset so that they can be separately seen. Also shown is a projection through the rotational 3D DSA volume.

For these cases the temporal resolution is reduced to 2–3 frames per second. However, this situation does not occur frequently due to the sparsity of the angiographic volume. Although the pixel matrix provided by the flat panel detectors used in 4D DSA suggest significantly lower voxel sizes than presently available with CTA or MRA, careful application of C-arm rotational calibration data will be required to achieve this potential, and additional validation is required to verify the expected resolution.

4D DSA has potential for significantly enhancing the capabilities of interventional C-arm systems. From a diagnostic perspective, the ability to rotate the acquired series of time frames provides a unique advantage over conventional DSA. The elimination of the problem of overlapping structures and the enhanced SNR provided by the constrained reconstruction that is used reopens the possibility of effective low-dose IV angiography.

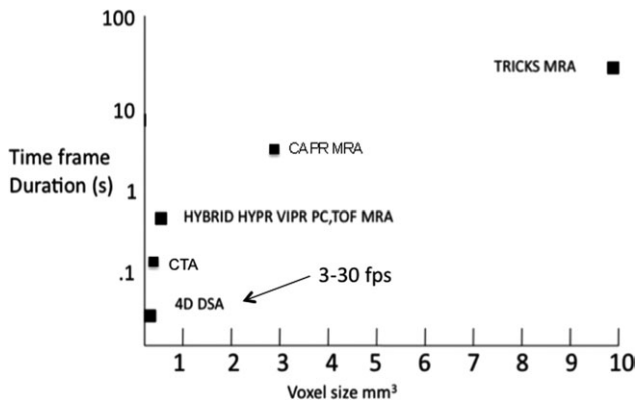

Figure 14. Spatial and temporal resolution of several techniques applied to cerebral angiography.

The 4D DSA time frames can also be used to provide simplified roadmaps for guidance of interventional devices. Due to limitations of C-arm motion there are often inaccessible fluoroscopic views, without which some interventions cannot be performed. Using a modified reconstruction related to the 4D DSA reconstruction, it is possible to provide fluoroscopic images that can be rotated to even inaccessible view angles without moving the C-arm gantry. This process, which we call omni-plane fluoroscopy, presently requires a bi-plane fluoroscopy system (Fig. 15). The temporal information from the two fluoroscopic views is used to embed the time dependence into the selected 3D roadmap, which can then be rotated in arbitrary directions showing the relationship of the vascular structures and the interventional device. Having access to a complete temporal library of roadmaps should reduce the number of contrast injections used during the interventional procedure, thus reducing radiation exposure and contrast dose.

A selected 3D roadmap and two fluoroscopic views are combined to embed the fluoroscopic information in the 3D vascular volume. Once this is done, the fluoroscopy can be viewed from any orientation without moving the C-arm gantrys. These results have been implemented in MatLab (MathWorks, Natick, MA) in a postprocessing mode. Graphics processing hardware implementation to permit real-time application is under way. This mode requires a bi-plane system.

DISCUSSION

There has been a steady progression of methods for time-resolved angiography over the past three decades. In the last decade there has been a particularly rapid acceleration in the ability of angiographic methods to combine high spatial and temporal resolution

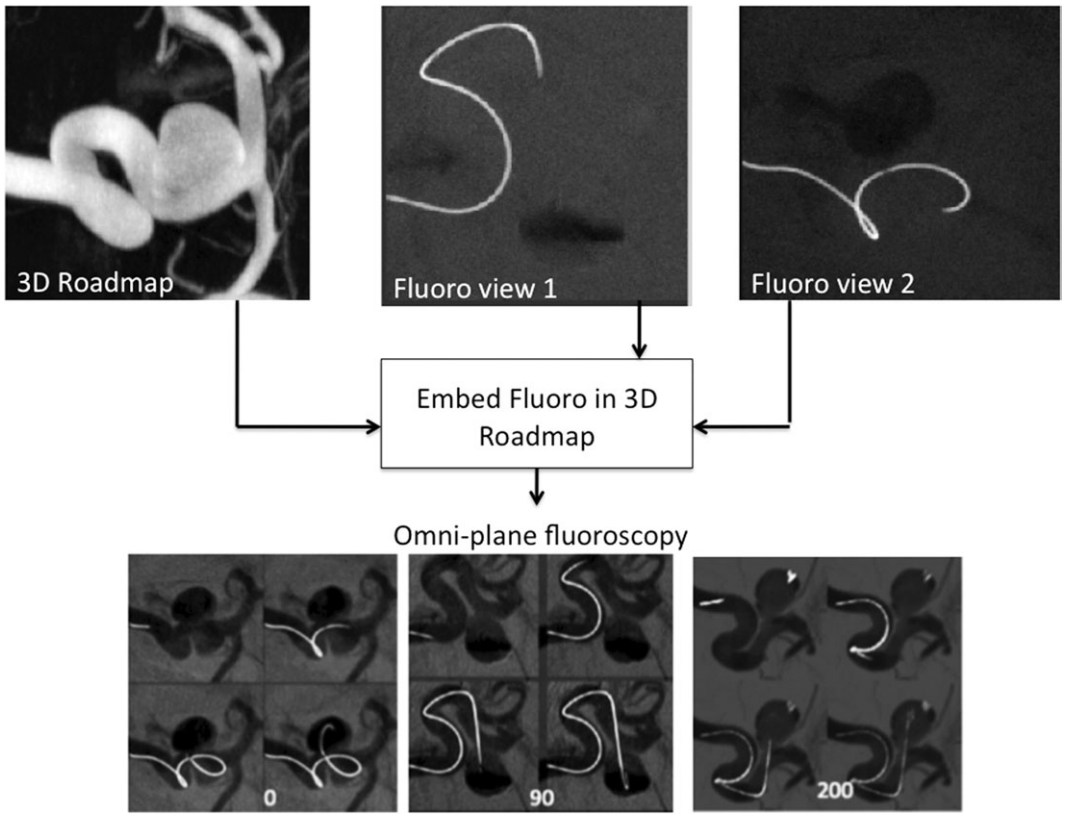

Figure 15. Schematic of omni-plane fluoroscopy.

while preserving SNR. The advent of parallel MRI has led to the acceleration of traditional Cartesian methods (44). The use of highly undersampled 3D radial acquisition (27) which can also be combined with parallel imaging leads to very high acceleration factors. The implementation of 3D radial imaging will require a major commitment from industry both in the implementation of required trajectory corrections and also in the processing in the larger amount of data generated in any given amount of time.

The traditional SNR loss associated with accelerated acquisition has been significantly reduced with the advent of constrained reconstruction techniques such as HYPR and its derivatives. It is our opinion that there is little reason not to apply this kind of processing to any time-resolved angiographic application. In selected applications like Hybrid MRA, acceleration factors on the order of 1000 have been achieved. The addition of compressed sensing methods can add another factor of five or so by reducing artifacts and permitting greater degrees of undersampling (48).

The ability to simultaneously provide high spatial and temporal resolution has opened the way for new application such as the noninvasive measurements of arterial pressure gradients and shear stress using phase contrast MRI with ECG gated time-resolved acquisition, providing exquisite information on flow dynamics. However, this application presents the highest requirements for data handling, with 36,000 images generated in some time-resolved examinations (eg, 30 3D volumes with 400 slices and three flow directions). Clearly, advanced visualization techniques will need to be developed to permit interpretation of these data.

Commercially, the implementation of advanced acceleration techniques is a lengthy process. At this point all major manufacturers have implemented 1D and 2D parallel imaging techniques which by now have undergone extensive validation. These have been used in conjunction with TRICKS and related techniques typically to improve spatial or temporal resolution. However, the implementations of techniques such as VIPR require detailed *k*-space corrections which, although they have been robustly implemented in university laboratories, require a substantial engineering effort to create reliable products. Compressed sensing and constrained reconstruction techniques such as HYPR should be easier to implement, but even for these primarily postprocessing techniques commercial availability will lag behind the reported academic studies.

Although the implementations are quite different in the case of 4D DSA, there is no question that the development of accelerated methods for MRA inspired the development of this technique. The additional speed and SNR provided by 4D DSA provides significant advantages of the original DSA method introduced 30 years ago. A combination of the early DSA method with retrospective electrocardiogram (ECG) sorting was used in early attempts to perform IV coronary angiography, but as with other IV DSA applications, overlap of structures was prohibitive.

Application of 4D DSA to intravenous coronary angiography is in its early stages.

Presently, work is also proceeding on the extension of 4D DSA to provide 4D perfusion measurements with subsecond temporal resolution. This requires significant modification of the algorithm shown in Figure 11 due to the need for more than just two projections.

In conclusion, it already seems quite probable that 4D DSA will provide significant dose savings in the interventional suite. The 4D fluoroscopy capabilities have the potential to ensure that patients will not have to be sent to surgery for lack of views presently inaccessible due to C-arm gantry motion restrictions. However, it will require some time to fully validate the technique and to identify the most important applications.

REFERENCES

1. Dos Santos R, Lamas AC, Caldas JP. Arteriographie des membres et de l'aorte Abdominale. Paris: Masson; 1931. p 11.
2. Caldas JP. Arteriographie en serie avec l'appareil radiocaroussel. J Radiol 1931;18:34–39.
3. Castellanos A, Pereiras R, Garcia A. La angiocardiografia radioopaqua. Arch Habana 1937;31:523–596.
4. Kelcz F, Mistretta CA. Absorption edge fluoroscopy using a 3-spectrum technique. Med Phys 1977;3:159–168.
5. Kruger RA, Mistretta CA, Lancaster J, et al. A digital video image processor for real-time subtraction imaging. Opt Eng 1978;17: 652–657.
6. Ovitt TW, Capp, MP, Christenson PC, et al. Intravenous angiography using digital video subtraction techniques. Am J Cardiol 1982;49:1365–1367.
7. Mistretta CA, Crummy AB, Strother CM. Digital angiography: a perspective. Radiology 1981:139:273–276.
8. Mistretta CA, Crummy AB. Diagnosis of cardiovascular disease by digital subtraction angiography. Science 1981;214:761–765.
9. Fahrig R, Fox AJ, Lownie S, Holdsworth DW. Use of a C-arm system to generate true three-dimensional computed rotational angiograms: preliminary in vitro and in vivo results. AJNR Am J Neuroradiol 1997;18:1507–1514.
10. Fahrig R, Moreau M, Holdsworth DW. Three-dimensional computed tomographic reconstruction using a C-arm mounted XRII: correction of image intensifier distortion. Med Phys 1997;24: 1097–1106.
11. Wedeen VJ, Meuli RA, Edelman RR, et al. Projective imaging of pulsatile flow with magnetic resonance. Science 1985;230:946–948.
12. Gullberg GT, Wehrli FW, Shimikawa A, Simons MA. MR vasculature imaging with a fast gradient focusing pulse sequence and reformatted images from transaxial sections. Radiology 1987; 165:241–246.
13. Keller PJ, Drayer BP, Fram EK, Williams KD, Doumoulin CL, Sousa SP. MR angiography with two dimensional acquisition and three dimensional display. Radiology 1989;173:527–532.
14. Laub GA, Kaiser WA. MR angiography with gradient motion refocusing. J Comput Assist Tomogr 1988;12:377–382.
15. Dumoulin CL, Souza SP, Walker MF, Wagle W. Three-dimensional phase contrast angiography. Magn Reson Med 1989;9:139–149.
16. Prince MR, Yucel EK, Kaufman JA, Harrison DC, Geller SC. Dynamic gadolinium-enhanced three dimensional abdominal MR arteriography. J Magn Reson Imaging 1993;3:877–881.
17. Foo TK, Saranathan M, Prince MR, Chenevert TL. Automated detection of bolus arrival and initiation of data acquisition in fast, three-dimensional, gadolinium-enhanced MR angiography. Radiology 1997;203:275–280.
18. Lee VS, Martin DJ, Krinsky GA, Rofsky NM. Gadolinium-enhanced MR angiography, artifacts and pitfalls. AJR Am J Roentgenol 2000;175:197–205.
19. Riederer SJ, Fain SB, Kruger DG, Busse RF. Real-time imaging and triggering of 3D contrast-enhanced MR angiograms using MR fluoroscopy. MAGMA 1999;8:196–206.
20. Wilman AH, Riederer SJ, King BF, Debbins JP, Rossman PJ, Ehman RL. Fluoroscopically triggered contrast-enhanced three-dimensional MR angiography with elliptical centric view order: application to the renal arteries. Radiology 1997;205:137–146.
21. Zur Y, Wood ML, Neuringer LJ. Spoiling of transverse magnetization in steady state sequences. Magn Reson Med 1991;21:251–263.
22. Van Vaals J, Brummer ME, Dixon WT, et al. Keyhole method for accelerating imaging of contrast agent uptake. J Magn Reson Imaging 1993;3:671–675.
23. Korosec FR, Frayne R, Grist TM, Mistretta CA. Time-resolved contrast-enhanced 3D MR angiography. Magn Reson Med 1996;36: 345–351.
24. Peters DC, Grist TM, Korosec FR, et al. Undersampled projection reconstruction applied to MR angiography. Magn Reson Med 2000;43:91–101.
25. Rasche V, deBoer RW, Holz D, Proska R. Continuous radial acquisition for dynamic MRI. Magn Reson Med 1995;34:754–761.
26. Scheffler K, Hennig J. Reduced circular field of view imaging. Magn Reson Med 1998;40:474–480.
27. Barger AV, Peters DC, Block WF, et al. Phase-contrast with interleaved undersampled projections. Magn Reson Med 200;43: 503–509.
28. Lum DP, Johnson KM, Paul RK, et al. Measurement of trans-stenotic pressure gradients in swine: comparison between retrospective ECG-gated 3D phase-contrast MRA and endovascular pressure-sensing guidewires. Radiology 2007;245:751–760.
29. Turk AS, Johnson KM, Lum D, et al. Physiological and anatomic assessment of a canine artery stenosis model with phase contrast with vastly undersampled isotropic projection imaging. AJNR Am J Neuroradiol 2007;28:111–115.
30. Moftakhar R, Aagaard-Kienitz B, Johnson K, et al. Noninvasive measurement of intra-aneurysmal pressure and flow pattern using phase contrast with vastly undersampled isotropic projection imaging. AJNR Am J Neuroradiol 2007;28:1710–1714.
31. Mistretta CA, Wieben O, Velikina J, et al. Highly constrained back projection for time-resolved MRI. Magn Reson Med 2006;55:30–40.
32. Webb AG, Liang ZP, Magin RL, Lauterbur PC. Applications of reduced-encoding MR imaging with generalized-series reconstruction (RIGR). J Magn Reson Imaging 1993;3:925–928.
33. Supanich M, Tao Y, Nett B, et al. Radiation dose reduction in time-resolved CT angiography using highly constrained back projection reconstruction. Phys Med Biol 2009;54:4575–4593.
34. Liu X, Primak AN, Krier JD, Yu L, Lerman LO, Mccullogh CH. Renal perfusion and hemodynamics: accurate in-vivo determination at CT with a 10 fold decrease in radiation dose and HYPR noise reduction. Radiology 2009;253:98–105.
35. Christian BT, Vandehey NT, Floberg J, Mistretta CA. Dynamic PET de-noising with HYPR processing. J Nucl Med 2010;51: 1147–1154.
36. Ge L, Kino A, Griswold M, Mistretta C, Carr J, Bebiao L. Myocardial perfusion MRI with sliding window conjugate gradient HYPR. Magn Reson Med 2009;62:835–839.
37. Johnson KM, Velikina J, Wu Y, Kecskemeti S, Wieben O, Mistretta CA. Improved waveform fidelity using local HYPR reconstruction (HYPR LR). Magn Reson Med 2008;59:456–462.
38. O'Halloran RL, Wen Z, Holmes JH, Fain SB. Iterative reconstruction of time-resolved images using highly constrained back-projection (HYPR). Magn Reson Med 2008;59:132–139.
39. Samsonov AA, Wieben O, Block WF. HYPRIT: generalized HYPR reconstruction by iterative estimation. In: Proc ISMRM Workshop on Non-Cartesian MRI, Sedona, AZ; 2007 (abstract).
40. Ge L, Kino A, Griswold A, Mistretta C, Carr JC, Li D. Myocardial perfusion MRI with sliding-window conjugate-gradient HYPR. Magn Reson Med 2009;62;835–839.
41. Candes EJ, Romberg J, Tao T. Robust uncertainty principles: exact signal reconstruction from highly incomplete frequency information. IEEE Inf Theory 2006;52:489–509.
42. Lustig M, Donoho D, Pauly JM. Sparse MRI: the application of compressed sensing for rapid MR imaging. Magn Reson Med 2007;58:1182–1195.
43. Velikina JV, Samsonov AA. HYPR-L0: a hybrid technique for CE MRA with extreme data undersampling factors. In: Proc 17th Annual Meeting ISMRM, Honolulu; 2009 (abstract 277).
44. Haider CR, Glockner J, Stanson AW, Reiderer S. Peripheral vasculature: high temporal- and spatial-resolution three-dimensional contrast-enhanced MR angiography. Radiology 2009;253: 831–843.

45. Trzasko JD, Haider CR, Borisch EA, Riederer SJ, Manduca A. Nonconvex compressive sensing with parallel imaging for highly accelerated 4D CE-MRA. In: Proc 18th Annual Meeting ISMRM, Stockholm; 2010 (abstract 347).
46. Johnson CP, Haider CR, Borish EA, Glockner JF, Riederer SJ. Time-resolved bolus chase MR angiography with real-time triggering of table motion. Magn Reson Med 2010;64:629–637.
47. Wang K, Holmes J, Busse R, et al. Interleaved variable density sampling with ARC parallel imaging and Cartesian HYPR for dynamic MR angiography. In: Proc Joint Annual Meeting ISMRM-ESMRMB, Stockholm; 2010 (abstract 352).
48. Velikina JV, Johnson KM, Wu YJ, Turski PA, Mistretta CA. PC HYPR FLOW. Magn Reson Imaging 2010;31:447–456.
49. Wu Y, Chang W, Johnson KM, et al. Fast whole-brain 4D contrast-enhanced MR angiography with velocity encoding using undersampled radial acquisition and highly constrained projection reconstruction: image-quality assessment in volunteer subjects. AJNR Am J Neuroradiol 2011;32:E47–50.
50. Miyazaki M, Sugiura S, Tateisi F, et al. Non-contrast-enhanced MR angiography using 3D ECG-synchronized half-Fourier fast spin echo. J Magn Reson Imaging 2000;12:776–783.
51. Takahashi J, Isono S, Miyazaki M, et al. Nonenhanced renal MRA using time-SLIP with 3D balanced SSFP: optimization of coronal acquisition. In: Proc 17th Annual Meeting ISMRM, Honolulu; 2009 (abstract 3900).
52. Edelman RR, Sheehan JJ, Dunkle E, Schindler N, Carr J, Koktzoglou I. Quiescent-interval single shot unenhanced magnetic resonance angiography of peripheral vascular disease: technical considerations and clinical feasibility. Magn Reson Med 2010;63:951–958.
53. Bi X, Weale P, Schmitt P, Zuehlsdorff S, Jerecic R. Non-contrast-enhanced four-dimensional (4D) intracranial MR angiography with 4D NATIVE. In: Proc 17th Annual Meeting ISMRM, Honolulu; 2009 (abstract 3259).
54. Bi X, Weale P, Schmitt P, Zuehlsdorff S, Jerecic R. Non-contrast-enhanced four-dimensional (4D) intracranial MR angiography: a feasibility study. Magn Reson Med 2010;63:835–841.
55. Yan L, Zhuo Y, An J, Wang J. Dynamic MR angiography and microvascular flow imaging with high temporal resolution using true FISP based spin tagging with alternating radiofrequency (TrueSTAR). In: Proc Joint Annual Meeting of ISMRM-ESMRMB, Stockholm; 2010 (abstract 1773).
56. Kimura T, Kitane S, Sueoka K. Non-contrast time resolved MR angiography combining multiple IR and N-1 subtraction arterial spin labeling technique. In: Proc Joint Annual Meeting of ISMRM-ESMRMB, Stockholm; 2010 (abstract 1440).
57. Johnson KM, Wieben O, Block WF, Mistretta CA. Accelerated time resolved inflow imaging with 3D radial bSSFP. In: Proc ISMRM Workshop on Data Sampling and Image Reconstruction, Sedona, AZ; 2009 (abstract).
58. Johnson KM, Wieben O, Turski P, Mistretta CA. Accelerated time resolved inflow with 3D multi-echo radial trajectories. In: Proc Joint Annual Meeting of ISMRM-ESMRMB, Stockholm; 2010 (abstract 3781).
59. Ishida F, Ogawa H, Simizu T, Kojima T, Taki W. Visualizing the dynamics of cerebral aneurysms with four-dimensional computed tomographic angiography. Neurosurgery 2005;57:460–471.
60. Mistretta C, Oberstar E, Davis B, Brodsky E, Strother CM. 4D-DSA and 4D fluoroscopy: preliminary implementation. In: Proc SPIE Conference on Medical Imaging, San Diego; 2009.